

Laboratory Investigation on the Behavior of Reef Breakwaters

Christos Antoniadis*

Coastal and Port Engineer/Rogan & Associates S.A., Athens, Greece

Abstract

An experimental investigation into the hydrodynamic behavior of reef breakwaters was carried out. The experiment aimed to provide full scale measurements of the main wave features at the front and rear of the breakwater, which have been analysed with variation of frequency and freeboard, for constant crest width and porosity. A series of tests was carried out at a 2-D wave flume. The analysis has shown that the reflection coefficient was a much more linear process than the transmission coefficient. The transmission coefficient was influenced mostly by the variation of the freeboard, in particularly, as the model became submerged.

Keywords: Reef breakwater; Submerged; Transmission; Dissipation; Reflection; Freeboard

Introduction

In this paper the performance of reef breakwaters was investigated. A reef breakwater is a low-crested homogeneous pile of stones without a filter layer or core and is allowed to be reshaped by wave attack. The initial crest height is just above the water level. Under severe wave conditions the crest height adjusts to a new equilibrium crest height. This equilibrium crest height and the corresponding transmission are the main design parameters [1].

Reef breakwaters are generally detached and parallel to the shore, with much overtopping. The mound of (graded) stones from which they are composed allows for the development of a dynamic stable profile, as opposed to low-crest or submerged breakwaters, which are nothing more than conventional, statically and stable rubble mounds [2-4]. Unfortunately, the performance of low-crested rubble mound structures, and particularly a reef breakwater, is not well documented or understood [5-9].

Since the cost of rubble mound increases exponentially with the height of the crest, the economic advantage of a low-crested structure, over a traditional breakwater that is infrequently overtopped, is apparent. Because the reef type breakwater is the state of the art in design simplicity it emerges as the optimum structure for many situations [10,11].

The geometric design of a reef breakwater is largely determined by the fact that marine equipment is normally required for construction. Sometimes construction is carried out with land-based equipment via a (temporary) causeway, but this approach is not favored, as it requires substantially more material handling. Reef breakwaters are generally built as part of a coastal defence scheme, and are mostly constructed in shallow water, with the consequences of shallow water breakwater design and construction [12].

In this paper, the behavior of reef type breakwaters was investigated by means of laboratory model. The importance of laboratory experiment is well known for scientific research, since experiments give rise to the opportunity to check on the accuracy of theoretical models, and also improve on the understanding of the physical processes involved in the theoretical model [13].

The main goal of the report was to investigate the influence of the variation of mean water level (submerged and not submerged model) and the variation of frequency, for random wave conditions, at wave reflection and transmission for reef type breakwaters. An observation

of the behavior of the dissipation of the reef type breakwaters was also included in this study.

Experimental Methods and Procedures

Wave flume

Three experiments with a total of 14 tests were carried out in a wave flume in the Brunel Laboratory. The flume had a length of 17.65 m, width of 0.90 m and was used with a working depth of 0.8 m. It had a 1:10 sloping section at the front and then followed by a 3.50 m flattening section reaching a final 1:10 sloping section. The flume bed was made by plastic. The sloping bed at the rear of the flume was reinforced by a wooden section in order to hold the weight of the model. Waves were generated by a hydraulic driven wave paddle system controlled via computer software. The system was capable of generating series of random waves. It has been shown that generating the wave in deep water reduces the magnitude of free log waves (induced by wave paddle) to the minimal. The wave motion generated by the wave paddle was repeatable therefore data collection at different location can be obtained through separate runs of each of the wave cases. Wave absorption was fully software driven using digital filters.

The reef breakwater model

The tests were conducted using a reef breakwater model. The model was placed, as mentioned above, at the end of the flume. It had a 14.27 m distance from the wave paddle system. The model had a front slope of 1:2, a crown height of 0.25 m, a crest width of 0.25 m and a rear slope of 1:1. The rocks had a diameter (D_{n50}) approximately 5 to 6 cm and an individual weight of 0.45 Kgr. Moreover, to improve the stability of the structure, a cottage wire was placed above the model. The dimensions details of the model and the wave flume can be seen in Figure 1.

During the tests, two white cylinders were used. They had 1.2 m length each with an inner and an outer diameter of 19 mm and 21 mm respectively. They were placed sidelong the model for checking if the

*Corresponding author: Christos Antoniadis, Coastal and Port Engineer/Rogan & Associates S.A., Athens, Greece, Tel: +306979708081; E-mail: cantoniadis79@hotmail.com

Received June 24, 2014; Accepted July 28, 2014; Published August 06, 2014

Citation: Antoniadis C (2014) Laboratory Investigation on the Behavior of Reef Breakwaters. J Coast Dev 17: 389. doi: [10.4172/1410-5217.1000389](https://doi.org/10.4172/1410-5217.1000389)

Copyright: © 2014 Antoniadis C. This is an open-access article distributed under the terms of the Creative Commons Attribution License, which permits unrestricted use, distribution, and reproduction in any medium, provided the original author and source are credited.

water would pass through the model and stabilize behind the structure without flowing back again, after it reflected at the sloping bed, causing increase in the volume of water behind the model and errors in readings. To check whether that would happen, a red dye was used.

The red dye was inserted into the water and found that the water flow through the cylinders from the “landward” to the “seaward” direction. As a result, the model proved safe for use.

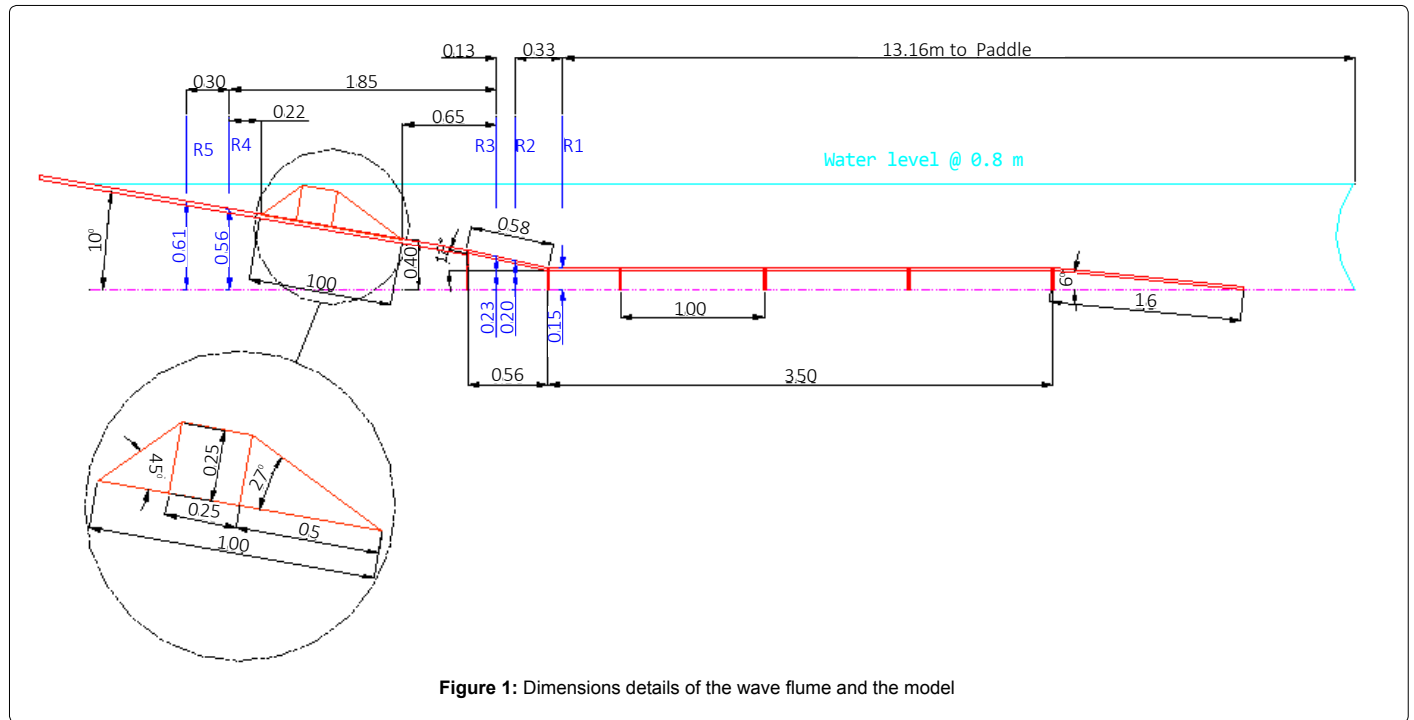


Figure 1: Dimensions details of the wave flume and the model

Experiment 1	Frequency(Hz)	Hi (m)	M.W.L. (m)	Freeboard (m)
Test 1	0.4	0.1	0.756	-0.044
Test 2	0.6			
Test 3	0.9			
Experiment 2	Frequency(Hz)	Hi (m)	M.W.L. (m)	Freeboard (m)
Test 1	0.4	0.1	0.795	-0.005
Test 2	0.6			
Test 3	0.8			
Test 4	0.9			
Test 5	1			
Experiment 3	Frequency(Hz)	Hi (m)	M.W.L. (m)	Freeboard (m)
Test 1	0.4	0.1	0.856	0.056
Test 2	0.6			
Test 3	0.8			
Test 4	0.9			
Test 5	1			

Table 1: Experimental test conditions

Mean Water Level at 0.756m (gauges1,2,3)												
f_p (Hz)	L_o (m)	d (m)			L (m)	d_t (m)	F (m)	H_{s1} (m)				
0.488	6.549	0.563	0.086	0.129	4.373	0.356	-0.044	0.061	1.033	0.369		-0.01
0.586	4.548	0.563	0.124	0.161	3.491	0.356	-0.044	0.091	0.688	0.306		-0.013
0.781	2.558	0.563	0.22	0.242	2.326	0.356	-0.044	0.084	0.553	0.274		-0.019
0.879	2.021	0.563	0.278	0.293	1.921	0.356	-0.044	0.085	0.487	0.214		-0.023
F/H_{s1}	C (m/s)	F/d_t	H_{s1}/L									
-0.717	2.135	-0.124	0.014									
-0.486	2.046	-0.124	0.026									
-0.527	1.817	-0.124	0.036									
-0.517	1.689	-0.124	0.044									

Table 2: Numerical presentation of K_r and various parameters for mean water level at 0.756 m.

Mean Water Level at 0.795 m (gauges 1, 2 and 3)												
f_p (Hz)	L_o (m)	d (m)	d/L_o	d/L	L (m)	d_t (m)	F (m)	H_{s1} (m)	ξ	K_r	F/L	
0.488	6.556	0.602	0.092	0.134	4.498	0.395	-0.005	0.055	1.091	0.359	-0.001	
0.586	4.547	0.602	0.132	0.168	3.573	0.395	-0.005	0.087	0.721	0.203	-0.001	
0.781	2.56	0.602	0.235	0.255	2.357	0.395	-0.005	0.078	0.573	0.164	-0.002	
0.879	2.021	0.602	0.298	0.31	1.942	0.395	-0.005	0.069	0.54	0.152	-0.003	
0.977	1.636	0.602	0.368	0.374	1.608	0.395	-0.005	0.069	0.488	0.131	-0.003	
F/H_{s1}	C (m/s)	F/d_t	H_s/L									
-0.091	2.195	-0.013	0.012									
-0.057	2.093	-0.013	0.024									
-0.064	1.841	-0.013	0.033									
-0.072	1.707	-0.013	0.036									
-0.073	1.571	-0.013	0.043									

Table 3: Numerical presentation of K_r and various parameters for mean water level at 0.795 m.

Mean Water Level at 0.795m (gauges 1,2,3)												
f_p (Hz)	L_o (m)	d (m)	d/L_o	d/L	L (m)	d_t (m)	F (m)	H_{s1} (m)	ξ	K_r	F/L	
0.488	6.556	0.663	0.101	0.142	4.663	0.456	0.056	0.053	1.114	0.408	0.012	
0.586	4.547	0.663	0.146	0.18	3.685	0.456	0.056	0.091	0.708	0.235	0.015	
0.781	2.56	0.663	0.259	0.276	2.402	0.456	0.056	0.075	0.584	0.203	0.023	
0.879	2.021	0.663	0.328	0.337	1.964	0.456	0.056	0.071	0.533	0.158	0.029	
0.977	1.636	0.663	0.405	0.409	1.618	0.456	0.056	0.069	0.486	0.142	0.035	
F/H_s	C (m/s)	F/d_t	H_s/L									
1.062	2.276	0.123	0.011									
0.616	2.159	0.123	0.025									
0.747	1.876	0.123	0.031									
0.788	1.726	0.123	0.036									
0.808	1.581	0.123	0.043									

Table 4: Numerical presentation of K_r and various parameters for mean water level at 0.856 m.

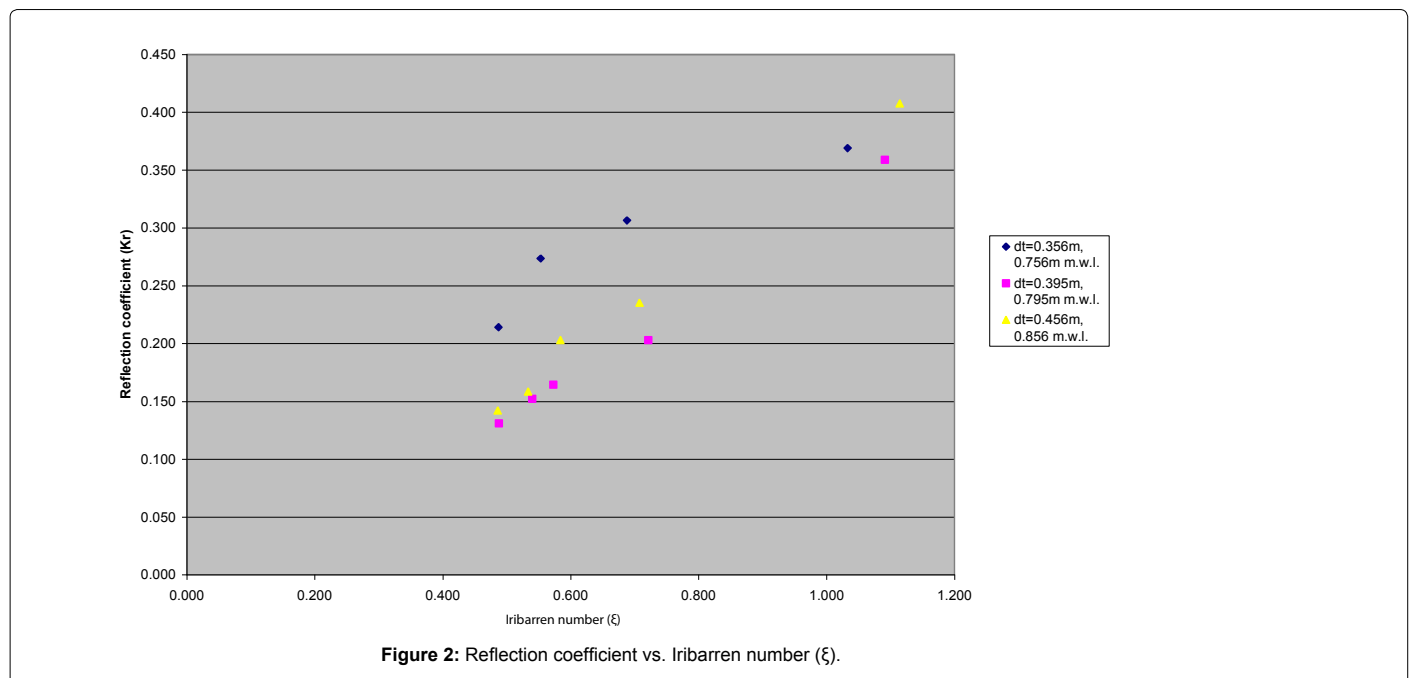


Figure 2: Reflection coefficient vs. Iribarren number (ξ).

The experimental tests

The reef breakwater model was tested using three mean water levels (m.w.l.), 0.756 m (Experiment 1), 0.795 m (Experiment 2) and 0.856 m (Experiment 3) for random wave conditions and for various frequencies. The crest width and the crest height were kept constant.

The peak frequencies (f_p) that were used, for each different mean water level, were the followings: 0.4 Hz, 0.6 Hz, 0.8 Hz, 0.9 Hz and 1.0 Hz. At 0.756 m m.w.l., the peak frequency equal to 1.0 Hz could not be used for the tests due to the fact that the wave paddle could not generate waves of this peak frequency for the given mean water level. Furthermore, the duration of the readings taken for each peak

frequency was 10 minutes. The generated wave height was adjusted to be 0.1 m. Table1 summarize all the experimental test conditions.

Instrumentation/Calibration

The vertical elevation of the water surface was measured using standard surface piercing wave gauges. To analyze wave reflection and transmission, five wave gauges were positioned near the structures registered with a frequency of 100 Hz (0.01 sample interval (sec)). Three gauges (namely R1, R2, and R3) were installed at the front of the

structure at a distance of 1.11 m, 0.78 m and 0.65 m respectively. The three gauges were used to measure the directional spectrum of waves composed of incident and reflected waves. Two wave gauges (R4, R5) were also installed at the rear of the structure to measure the directional spectrum of waves composed of transmitted waves. R4 and R5 had a 0.22 m and 0.52 m distance respectively, from the model. The location of the gauges can be seen in Figure 1. All the gauges were calibrated for all the tests. The method that was used for the calibration of the gauges was the following: Data was collected for duration of 100 seconds for

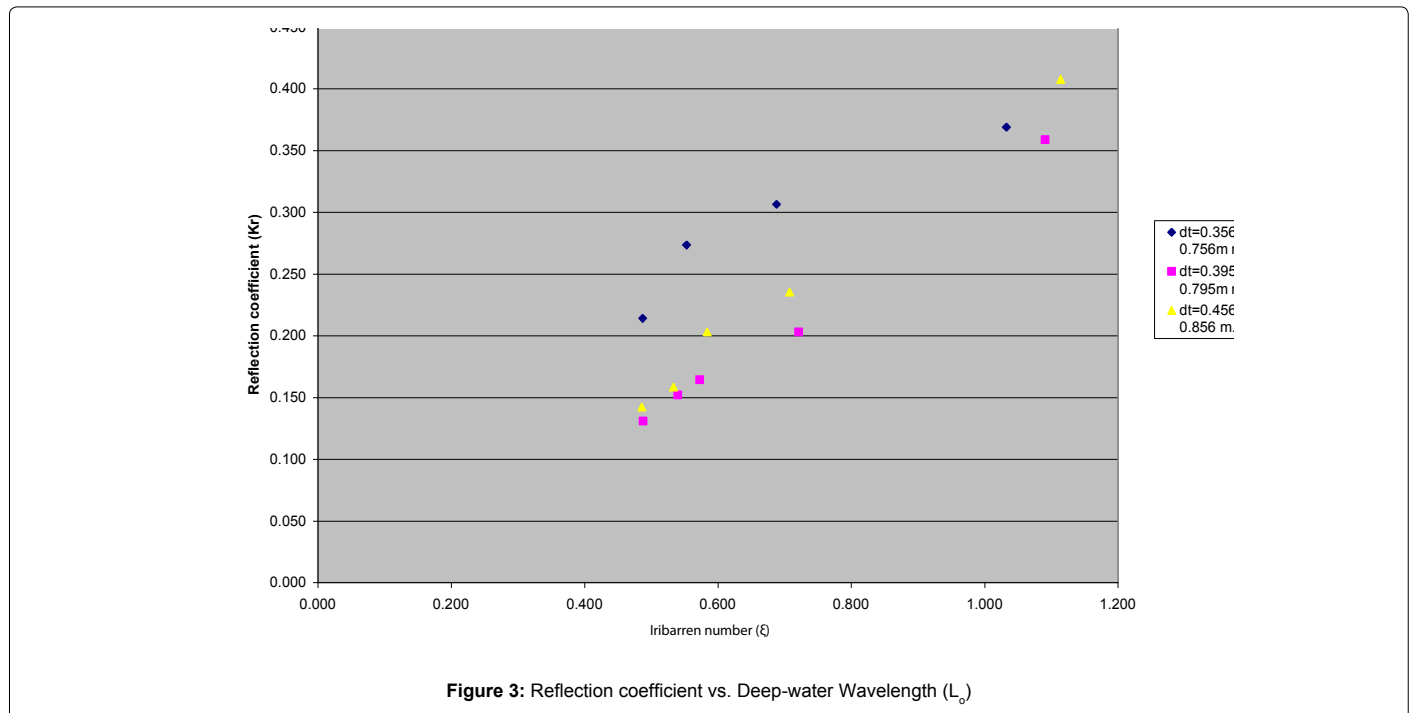


Figure 3: Reflection coefficient vs. Deep-water Wavelength (L_d)

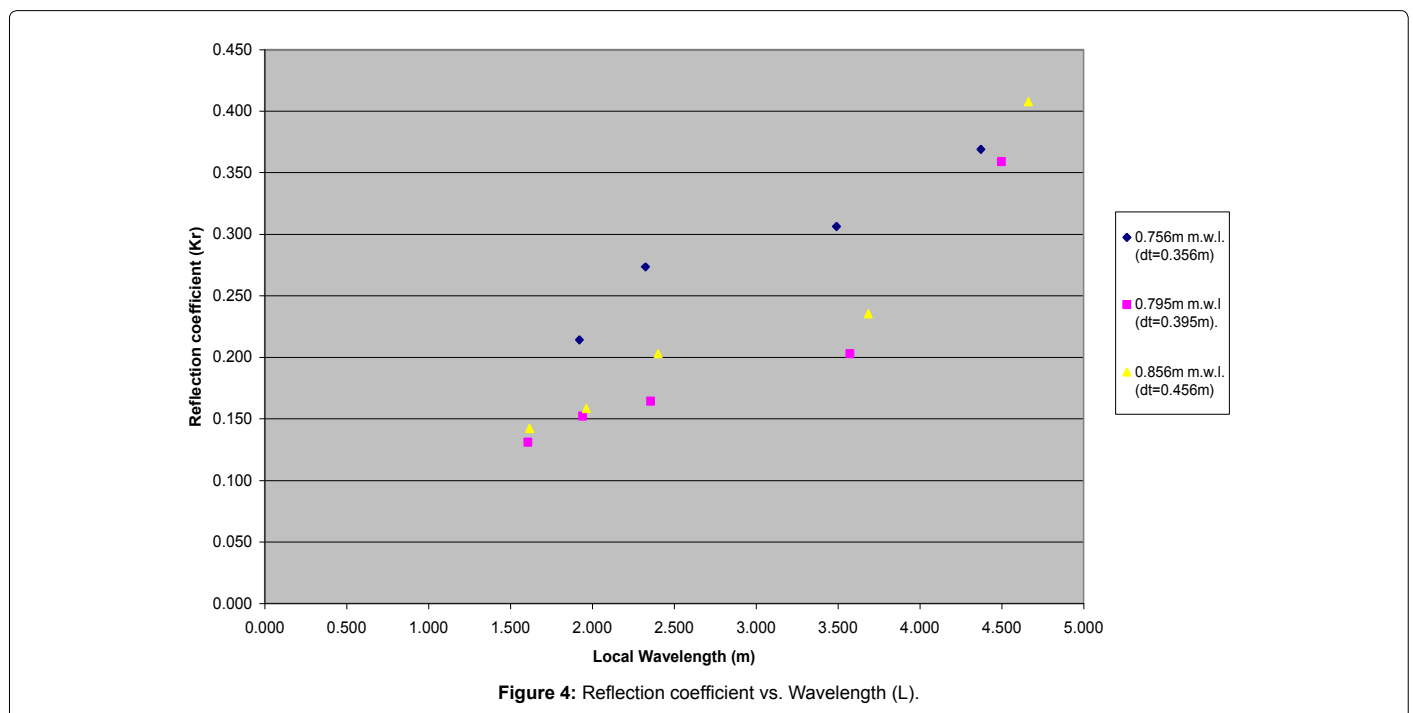


Figure 4: Reflection coefficient vs. Wavelength (L).

the still position of the gauges (zero level), then for the upward position (moved 50 mm upwards) and at last for the downward position (moved 50 mm downwards from the zero level). The collected data was measured in voltage units. The calibration of the gauges was carried out and checked for its accuracy, by plotting graphs of Elevation vs. Voltage, every time that the mean water level was changed.

Results

The data obtained from the experiment was analysed and the

results are presented here. The reflection coefficient (K_r) as a function of frequency was estimated from the spectral densities of the incident and the reflected wave fields. The reflection coefficient was investigated at the gauges 1-3. The transmission coefficient (K_t) was estimated similarly (incident and transmitted wave fields). The transmission coefficient was investigated at the gauges 4-5.

Effects of various parameters on reflection coefficient

The numerical presentation of K_r and the various parameters, for

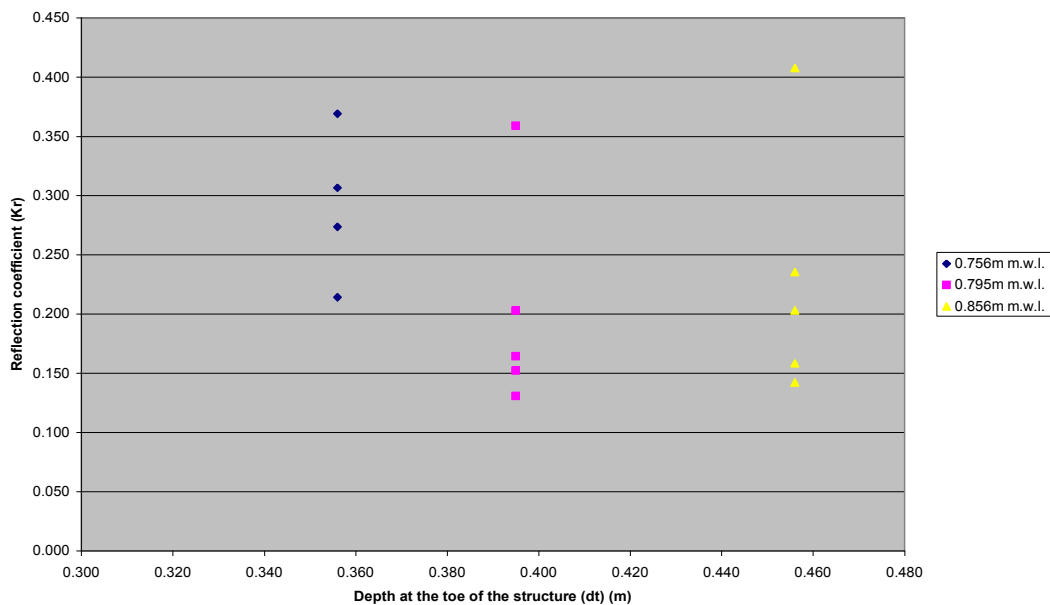


Figure 5: Reflection coefficient vs. Depth at the toe of the structure (d_t).

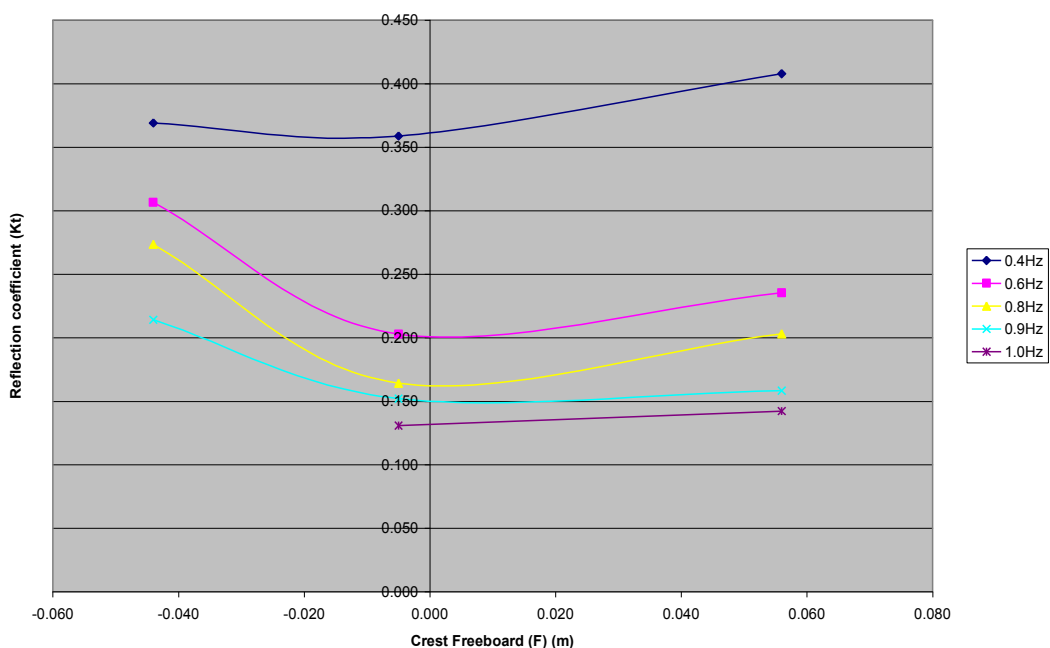


Figure 6: Reflection coefficient vs. Crest Freeboard (F).

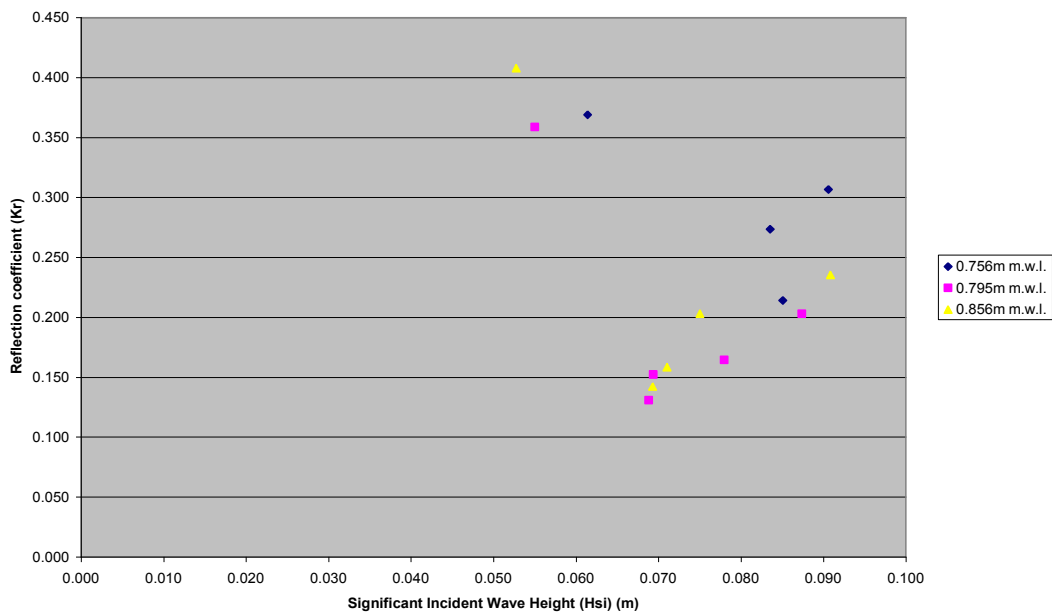


Figure 7: Reflection coefficient vs. significant incident wave height (H_s).

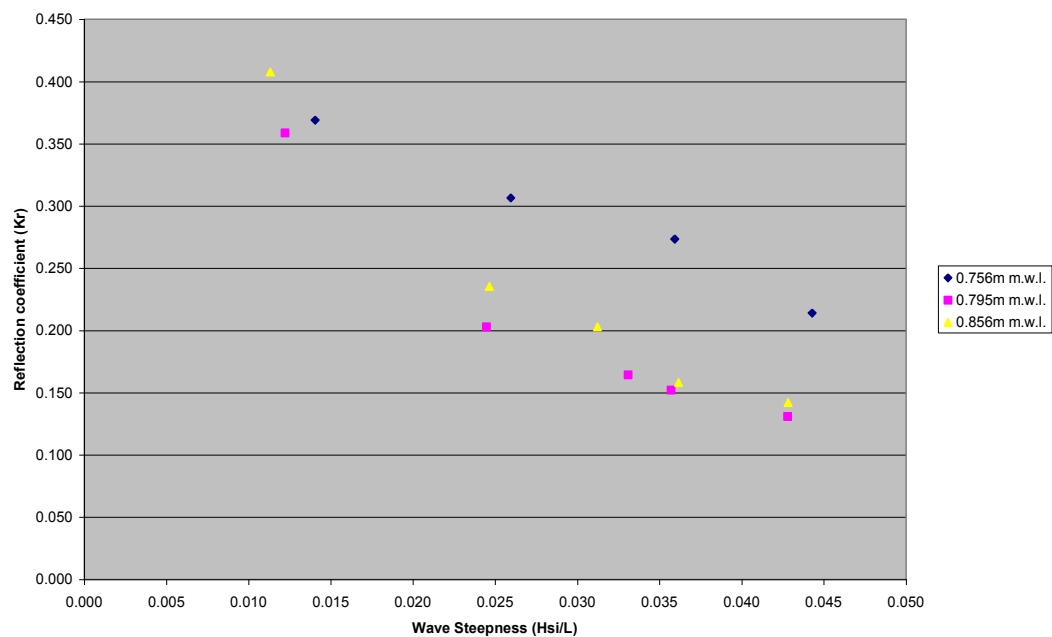


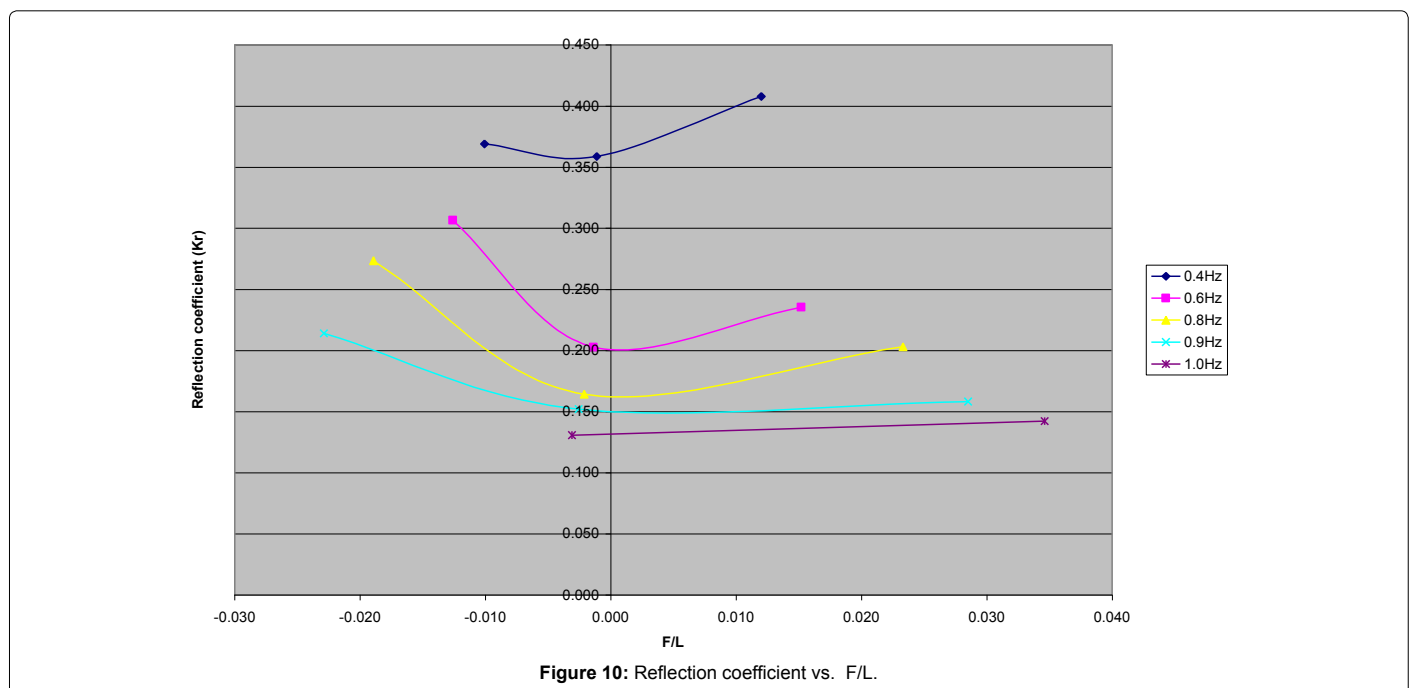
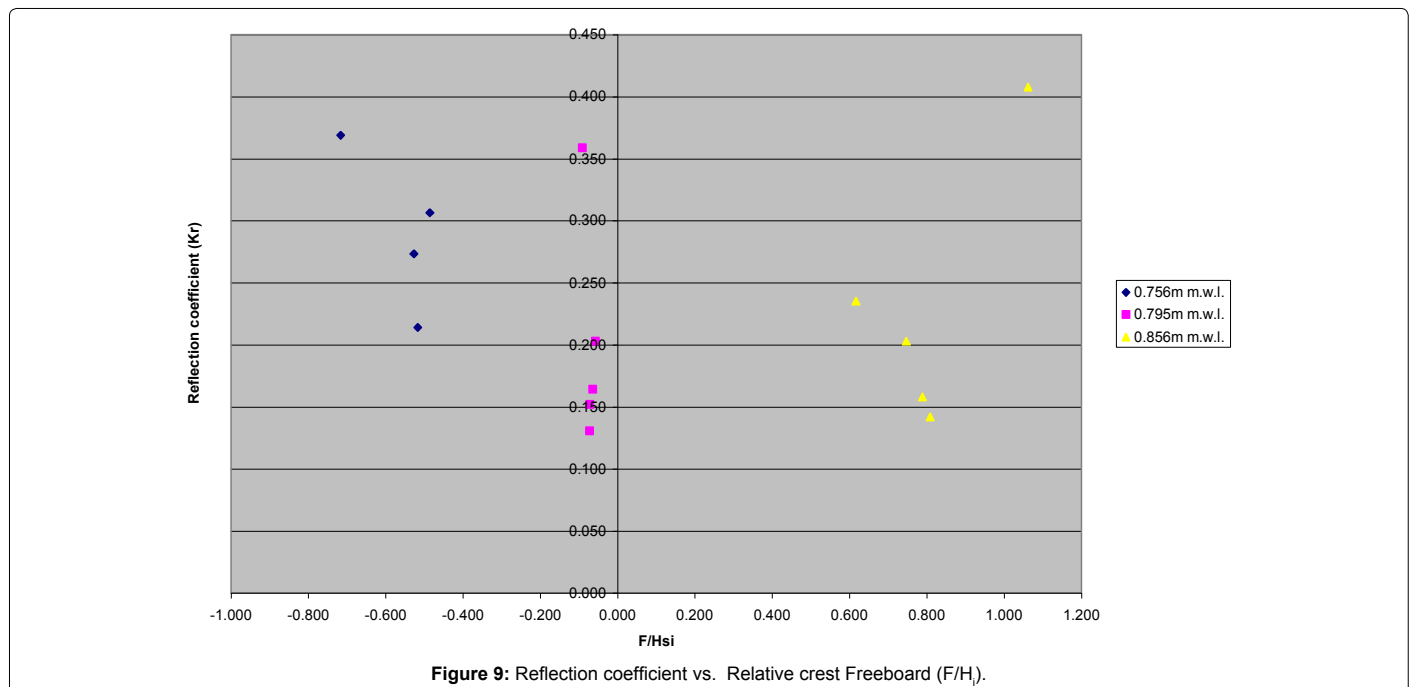
Figure 8: Reflection coefficient vs. Wave Steepness (H_s/L).

each mean water level, can be seen in Tables 2-4. At Tables 2-4, the peak frequency (f_p), the wavelength for deep water L_0 , the water depth at the gauges (d), the wavelength (L), the water depth measured at the toe of the structure (d_t), the crest freeboard (F), the incident wave height (H_{si}), the iribarren number (ξ), relative crest freeboard (F/H_{si}), relative depth of crest freeboard (F/d_t), wave steepness (H_{si}/L) and celerity (C) can be also seen.

The reflection coefficient is affected from various parameters, most notably from the Iribarren number (ξ). The reflection coefficient

was plotted against the Iribarren number using results from different depth at the toe of the structure and consequently different mean water level (shown in Figure 2). It was found that K_r was proportional to ξ . Moreover, a large scatter of the data was been noticeable at the initial values of Iribarren number.

The behavior of the reflection coefficient was observed in Figures 3-4 where it was plotted initially against the deep water wavelength (L_0) and then against the wavelength (L) at the gauges 1, 2 and 3. K_r was systematically increasing in direct relationship with the increase of the



deep water wavelength- L_o (and wavelength- L). The maximum values of K_r for different m.w.l. were close to each other with a maximum value of K_r at 0.856 m m.w.l.

Inspection of Figures 5 and 6 showed that the relationship between the reflection coefficient and the depth of the toe of the structure and also with the relative crest freeboard had similar results. In Figure 5, K_r seemed to decrease as d_t increased until it reached a value of d_t ($d_t=0.395$ m) where the model became submerged. After this value K_r started to increase. The same results can also be seen in Figure 6 for

different frequencies where the value of $d_t=0.395$ m corresponded to the value of $F=-0.05$.

The reflection was also plotted against the significant incident wave height (H_{si}) (in Figure 7) to identified the relationship between them. It was found that K_r was almost proportional to H_{si} . The reflection coefficient increased as the significant incident wave height increased, with the exception of values of H_{si} which corresponded to the frequency equal to 0.4 Hz.

The relationship of the reflection coefficient with the wave steepness

Mean Water Level at 0.756m (gauge 4)											
f_p (Hz)	Lo (m)	d (m)	d/L0	d/L	L(m)	dt(m)	F (m)	Hsi (m)	ξ	K_t	F/L
0.488	6.556	0.235	0.036	0.078	2.997	0.395	-0.005	0.055	1.091	0.357	-0.002
0.586	4.547	0.235	0.052	0.096	2.446	0.395	-0.005	0.087	0.721	0.289	-0.002
0.781	2.56	0.235	0.092	0.134	1.752	0.395	-0.005	0.078	0.573	0.306	-0.003
0.879	2.021	0.235	0.116	0.155	1.514	0.395	-0.005	0.069	0.54	0.302	-0.003
0.977	1.636	0.235	0.144	0.178	1.319	0.395	-0.005	0.069	0.488	0.28	-0.004
F/Hs _i	C (m/s)	F/dt	Hs/L								
-0.091	1.462	-0.013	0.018								
-0.057	1.434	-0.013	0.036								
-0.064	1.369	-0.013	0.045								
-0.072	1.331	-0.013	0.046								
-0.073	1.288	-0.013	0.052								

Table 5: Numerical presentation of K_t and various parameters for mean water level at 0.795 m.

Mean Water Level at 0.856m (gauge 4)											
f_p (Hz)	Lo (m)	d (m)	d/L0	d/L	L(m)	dt(m)	F (m)	Hsi (m)	ξ	K_t	F/L
0.488	6.556	0.296	0.045	0.089	3.328	0.456	0.056	0.053	1.114	0.455	0.017
0.586	4.547	0.296	0.065	0.109	2.705	0.456	0.056	0.091	0.708	0.48	0.021
0.781	2.56	0.296	0.116	0.155	1.913	0.456	0.056	0.075	0.584	0.459	0.029
0.879	2.021	0.296	0.146	0.181	1.639	0.456	0.056	0.071	0.533	0.475	0.034
0.977	1.636	0.296	0.181	0.209	1.418	0.456	0.056	0.069	0.486	0.491	0.039
F/Hs _i	C (m/s)	F/d _i	Hs/L								
1.062	1.624	0.123	0.016								
0.616	1.585	0.123	0.034								
0.747	1.494	0.123	0.039								
0.788	1.441	0.123	0.043								
0.808	1.385	0.123	0.049								

Table 6: Numerical presentation of K_t and various parameters for mean water level at 0.856 m.

Mean Water Level at 0.795m (gauge 4)											
f_p (Hz)	Lo (m)	d (m)	d/L0	d/L	L(m)	dt(m)	F (m)	Hsi (m)	ξ	K_t	F/L
0.488	6.556	0.185	0.028	0.069	2.681	0.395	-0.005	0.055	1.091	0.789	-0.002
0.586	4.547	0.185	0.041	0.084	2.205	0.395	-0.005	0.087	0.721	0.596	-0.002
0.781	2.56	0.185	0.072	0.116	1.589	0.395	-0.005	0.078	0.573	0.518	-0.003
0.879	2.021	0.185	0.092	0.133	1.389	0.395	-0.005	0.069	0.54	0.539	-0.004
0.977	1.636	0.185	0.113	0.152	1.219	0.395	-0.005	0.069	0.488	0.549	-0.004
F/H _{si}	C (m/s)	F/d _i	H _{si} /L								
-0.091	1.309	-0.013	0.021								
-0.057	1.292	-0.013	0.04								
-0.064	1.241	-0.013	0.049								
-0.072	1.221	-0.013	0.05								
-0.073	1.191	-0.013	0.056								

Table 7: Numerical presentation of K_t and various parameters for mean water level at 0.795 m.

Mean Water Level at 0.856m (gauge 5)											
f_p (Hz)	Lo (m)	d (m)	d/L0	d/L	L(m)	dt(m)	F (m)	Hsi (m)	ξ	K_t	F/L
0.488	6.556	0.246	0.038	0.081	3.052	0.456	0.056	0.053	1.114	0.792	0.018
0.586	4.547	0.246	0.054	0.098	2.505	0.456	0.056	0.091	0.708	0.235	0.022
0.781	2.56	0.246	0.096	0.138	1.785	0.456	0.056	0.075	0.584	0.781	0.031
0.879	2.021	0.246	0.122	0.159	1.545	0.456	0.056	0.071	0.533	0.763	0.036
0.977	1.636	0.246	0.15	0.184	1.339	0.456	0.056	0.069	0.486	0.762	0.042
F/Hs _i	C (m/s)	F/dt	Hs/L								
1.062	1.489	0.123	0.017								
0.616	1.468	0.123	0.036								
0.747	1.394	0.123	0.042								
0.788	1.358	0.123	0.046								
0.808	1.308	0.123	0.052								

Table 8: Numerical presentation of K_t and various parameters for mean water level at 0.856 m.

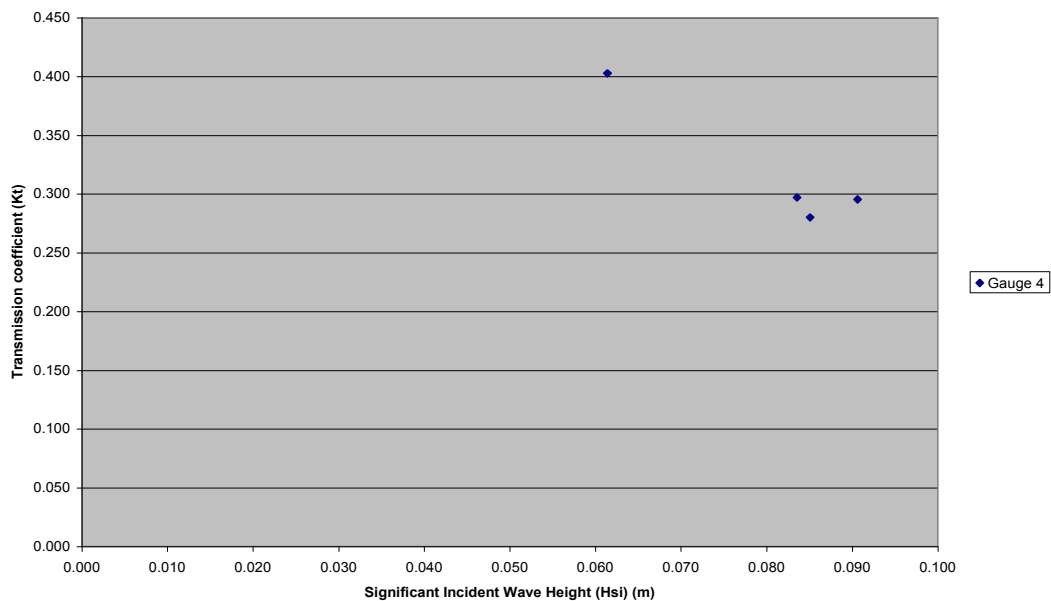


Figure 11: Transmission coefficient vs. Incident Wave Height (H_s) at 0.756 m m.w.l.

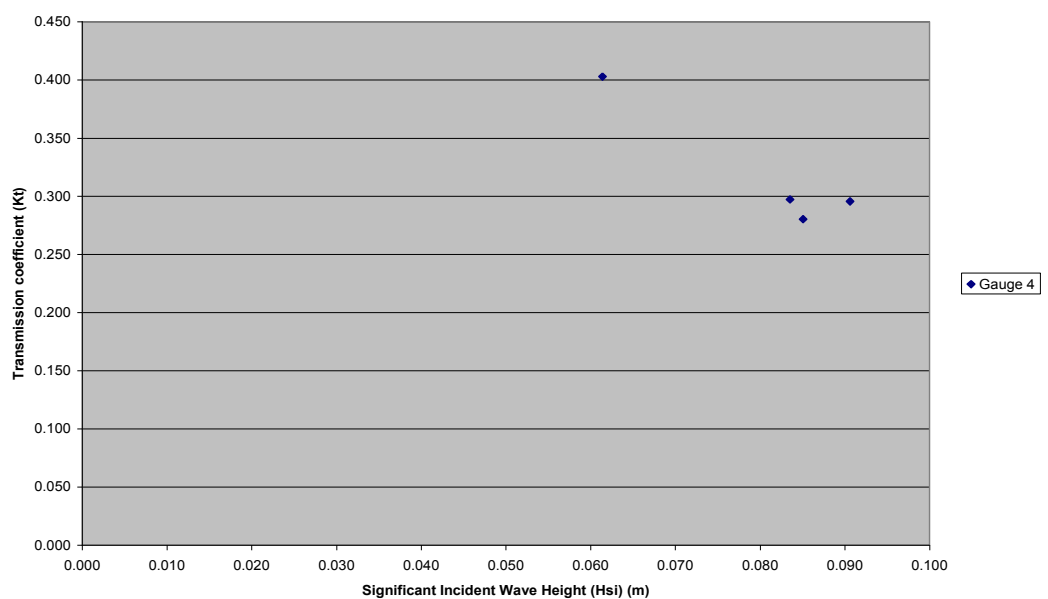


Figure 12: Transmission coefficient vs. Incident Wave Height (H_s) at 0.795 m m.w.l.

(H_{si}/L) can be described as inverse proportional. The reflection coefficient decreased as the wave steepness increased. Similarity between 0.795 m and 0.856 m m.w.l. was obtained when their values of K_r against H_{si}/L were very close to each other. In Figure 8, the plot of the reflection coefficient against the wave steepness for the three mean water levels can be seen.

The relationship of K_r and F/H_{si} can be seen in Figure 9. The reflection coefficient seemed to be inverse proportional to F/H_{si} with an exception at $f=0.4$ Hz (at 0.856 m m.w.l.) where K_r took a very large value. It can be noticed that when F/H_{si} became approximately zero, all

influence of the significant wave height was lost which lead to a large scatter in the graph at $F/H_{si} \approx 0$. Similar results were obtained for F/L (Figure 10) where the increase of K_r after $F/L \approx 0$ became smoother as the frequencies increased.

Effects of various parameters on transmission coefficient

The numerical presentation of K_t and the various parameters, for each mean water level and for each transmission gauge (R4, R5), can be seen in Tables 4-8.

The government parameters related to transmission are: the

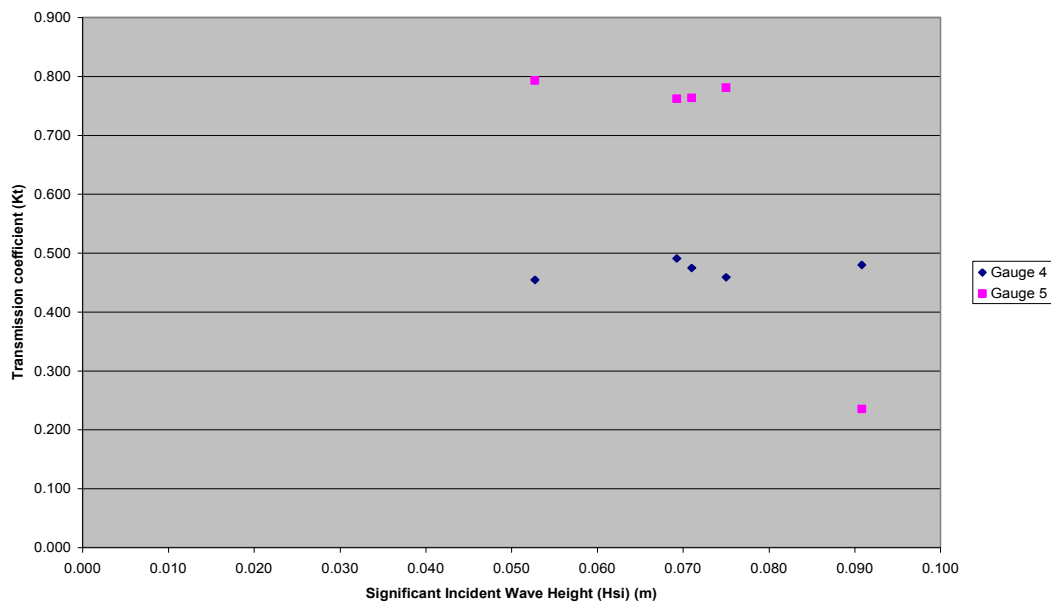


Figure 13: Transmission coefficient vs. Incident Wave Height (H_i) at 0.856 m m.w.l.

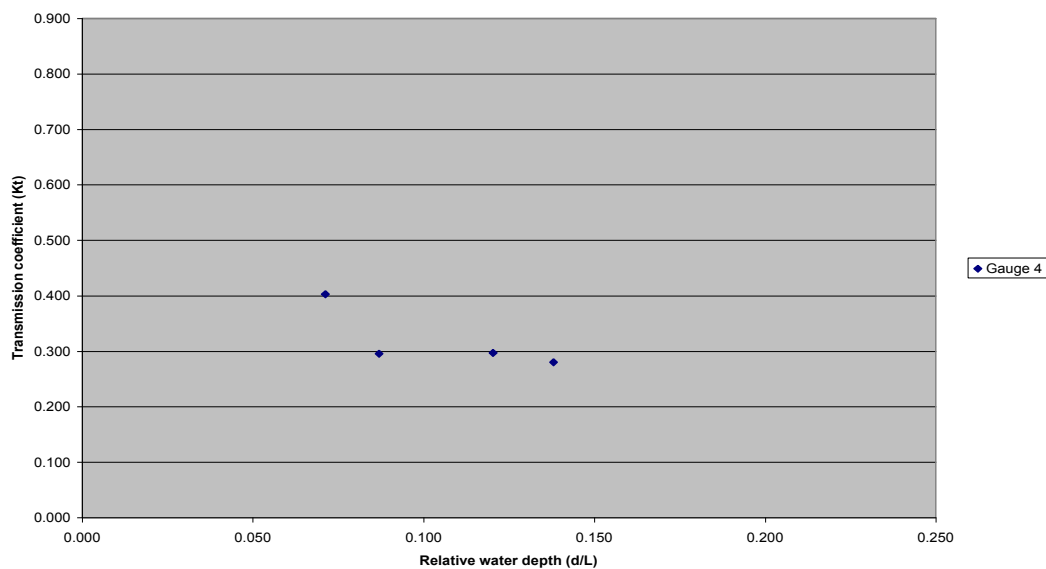


Figure 14: Transmission coefficient vs. Relative Water Depth (d/L) at 0.756 m m.w.l.

structure geometry, principally, the relative crest freeboard, crest width and water depth, permeability, and on the wave conditions, principally, the wave height and period. Due to the fact that the structure geometry, crest width and permeability remained constant, the transmission and especially its coefficient would fluctuate in relationship with the rest parameters. Consequently, the relationship between K_t (for both gauges- R4 & R5) and incident wave height (H_i), wave period (T) (already explained previously), relative water depth (d/L), wavelength (L) at R4 and R5, deep water wavelength (L_o), wave steepness (H_i/L), relative crest freeboard (F/H_i), F/L , crest freeboard (F) and relative depth of crest freeboard (F/d_i) was investigated.

The relationship between the transmission coefficient and the Significant Incident Wave Height (H_{si}) is shown in Figures 11-13. It

can be observed that the transmission coefficient was proportional to the increase of the significant incident wave height. However, when the model became submerged (0.856 m m.w.l.) K_t became inversely proportional to the increase of H_{si} .

In Figures 14-16 the transmission coefficient was plotted against the relative water depth (d/L). At 0.756 m m.w.l. the K_t was inversely proportional to the increase of the d/L . This behavior continued at 0.795 m m.w.l. as well, with an exception from the results taken from gauge 5 at which the K_t started to increase after $d/L=0.138$. At 0.856 m m.w.l. the results taken from gauge 4 showed that K_t start to increase as d/L increased. However, this was inverse proportional with the results taken from gauge 5 (K_t decreased as d/L increased).

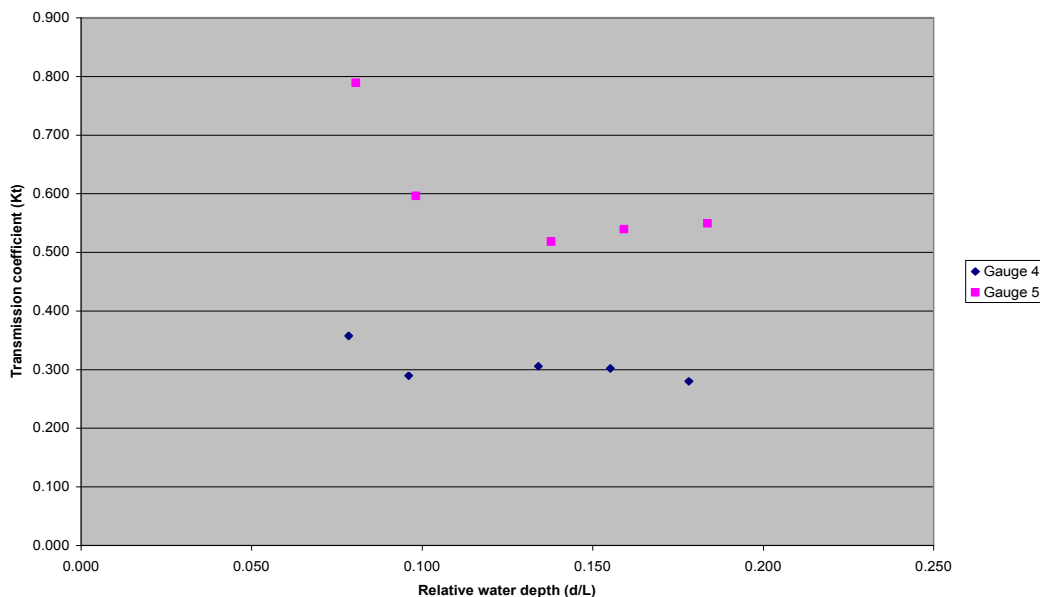


Figure 15: Transmission coefficient vs. Relative Water Depth (d/L) at 0.795 m m.w.l.

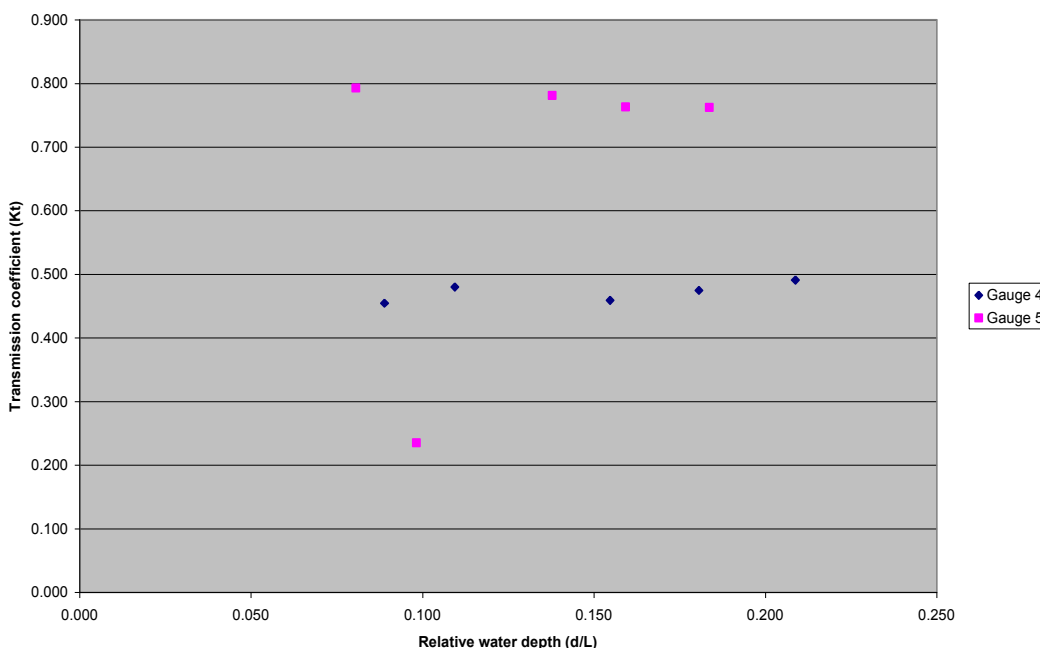


Figure 16: Transmission coefficient vs. Relative Water Depth (d/L) at 0.856 m m.w.l.

Furthermore, the effect of deep water wavelength (L_o) and wavelength (L) at gauges 4 and 5, on the transmission coefficient showed to be the same. Tables 4-8 showed that K_t was, in general, proportional with the increase of L and L_o until the model became submerged. Therefore at 0.856 m m.w.l. the transmission coefficient became inversely proportional to both of these parameters. The only exception to this behavior was the value of K_t (at gauge 5) corresponding to $f=0.6$ Hz for 0.856 m m.w.l.

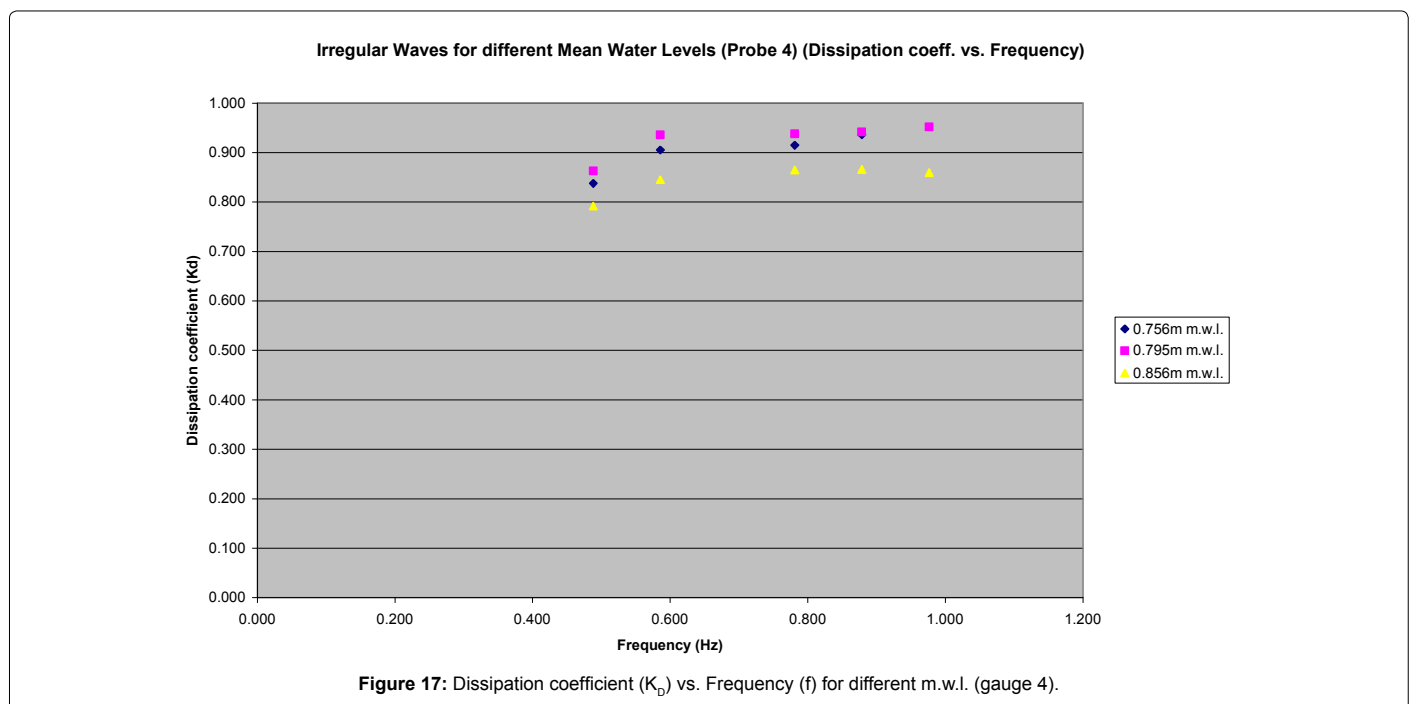
On the other hand, the effect of the transmission coefficient on the wave steepness (H_{st}/L) showed inverse results. As it is shown in

the numerical presentation, the K_t was inversely proportional to H_{st}/L for both gauges for 0.756 m and 0.795 m m.w.l. At 0.856 m m.w.l. the results taken from gauge 5 show that K_t continued to have an inversely proportional effect to the wave steepness, however the results taken from gauge 4 showed K_t to be smoothly proportional to H_{st}/L .

Observation of the behavior of K_t with respect to crest freeboard (F), relative depth of crest freeboard (F/d_c), relative crest freeboard (F/H_{st}) and F/L lead to similar conclusions. K_t was proportional to the increase of those parameters. As these parameters increased, the transmission coefficient increased having a large scatter at values where

Mean Water Level at 0.756m (gauge 4)					
Frequencies	Reflection coeff.	Transmission coeff.	Dissipation coeff.	Freeboard (m)	ξ
0.488	0.369	0.403	0.838	-0.044	1.033
0.586	0.306	0.296	0.905	-0.044	0.688
0.781	0.274	0.297	0.915	-0.044	0.553
0.879	0.214	0.28	0.936	-0.044	0.487
Mean Water Level at 0.795m (gauge 4)					
Frequencies	Reflection coeff.	Transmission coeff.	Dissipation coeff.	Freeboard (m)	ξ
0.488	0.359	0.357	0.862	-0.005	1.091
0.586	0.203	0.289	0.936	-0.005	0.721
0.781	0.164	0.306	0.938	-0.005	0.573
0.879	0.152	0.302	0.941	-0.005	0.54
0.977	0.131	0.28	0.951	-0.005	0.488
Mean Water Level at 0.795m (gauge 5)					
Frequencies	Reflection coeff.	Transmission coeff.	Dissipation coeff.	Freeboard (m)	ξ
0.488	0.359	0.789	0.499	-0.005	1.091
0.586	0.203	0.596	0.777	-0.005	0.721
0.781	0.164	0.518	0.84	-0.005	0.573
0.879	0.152	0.539	0.828	-0.005	0.54
0.977	0.131	0.549	0.825	-0.005	0.488
Mean Water Level at 0.856m (gauge 4)					
Frequencies	Reflection coeff.	Transmission coeff.	Dissipation coeff.	Freeboard (m)	ξ
0.488	0.408	0.455	0.792	0.056	1.114
0.586	0.235	0.48	0.845	0.056	0.708
0.781	0.203	0.459	0.865	0.056	0.584
0.879	0.158	0.475	0.866	0.056	0.533
0.977	0.142	0.491	0.859	0.056	0.486
Mean Water Level 0.856m (gauge 5)					
Frequencies	Reflection coeff.	Transmission coeff.	Dissipation coeff.	Freeboard (m)	ξ
0.488	0.408	0.792	0.453	0.056	1.114
0.586	0.235	0.235	0.943	0.056	0.708
0.781	0.203	0.781	0.591	0.056	0.584
0.879	0.158	0.763	0.627	0.056	0.533
0.977	0.142	0.762	0.632	0.056	0.486

Table 9: Numerical results of the analysis of the dissipation coefficient (K_D) for diff. m.w.l.



F was approximately equal to zero.

A comparison between the numerical presentation of both coefficients (K_r , K_t) reveals that the celerity was inversely proportional to the increase of frequency and also greater at gauges 1, 2, 3 than at gauges 4 and 5. Finally, the values of celerity increased as the mean water level increased.

Effects of various parameters on dissipation coefficient

It is known that the equation of energy balance can be derived by

the coefficients of reflection, transmission and dissipation [14]:

$$K_r^2 + K_t^2 + K_D = 1 \tag{1}$$

where,

K_r = reflection coefficient (H_r/H_i);

K_t =transmission coefficient (H_t/H_i); and

K_D =dissipation coefficient (E_d/E_i)

where,

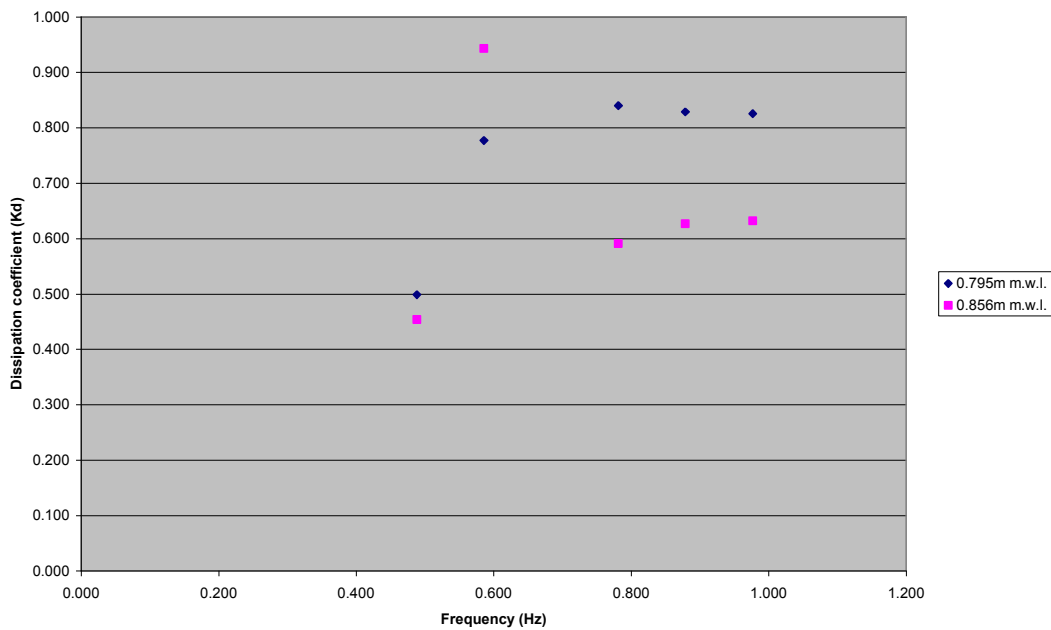


Figure 18: Dissipation coefficient (K_D) vs. Frequency (f) for different m.w.l. (gauge 5).

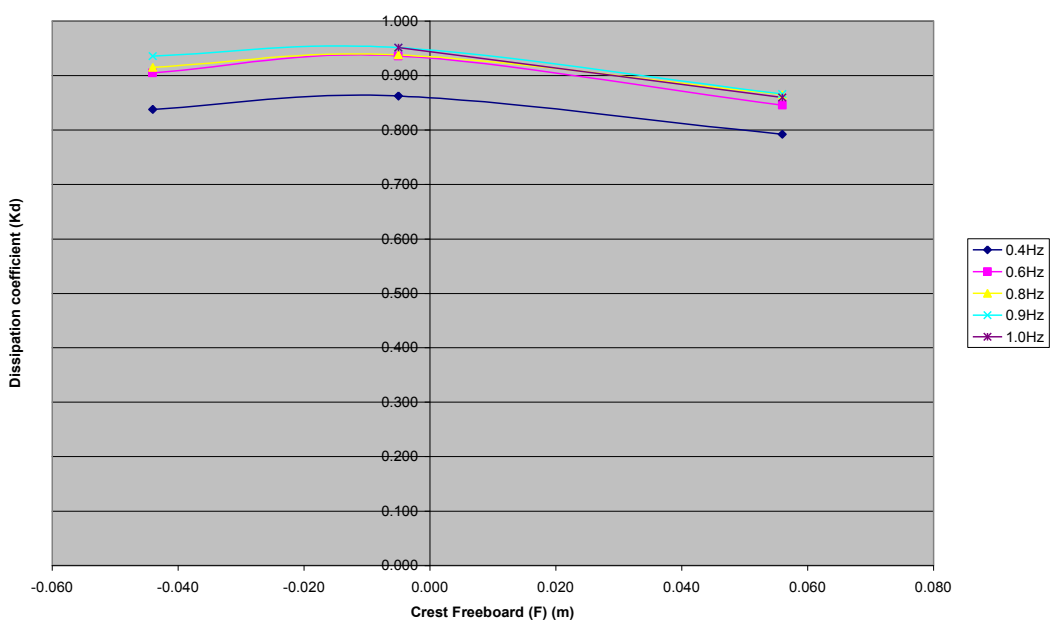


Figure 19: Dissipation coefficient (K_D) vs. Crest Freeboard (F) for different frequencies (gauge 4).

H_i = incident wave height at the seaside; and

H_t = transmitted wave height at the lee side.

H_r = reflected wave height

The dissipation coefficient was calculated for all the different frequencies and all the different mean water levels and it was observed that to have high values. The numerical results of that calculation (for both R4 and R5 separately) can be seen in Table 9. Figures 17-18 showed, for both gauges, that K_D had a smooth increase as frequency increased. Moreover, it can be concluded that after a point ($f=0.6$ Hz) was reached, that the increase stabilized to an almost constant value of

K_t with respect to the increase of frequency. However, the dissipation coefficient, which was calculated from the results taken from gauge 5, shows one changing point of its behavior at $f=0.6$ Hz at 0.856 m m.w.l.

From the observation of Figures 19-20 where the dissipation coefficient was plotted against the relative crest freeboard, it can be seen that K_D increased as F increased until a value of F , approximately equal to 0, was reached after which it started to decrease. Once more, the dissipation coefficient from gauge 5 showed one changing point of its general behavior at $f=0.6$ Hz.

Finally, in Figures 21-22 where K_D was plotted against Iribarren number (ξ), it can be seen that the dissipation coefficient was inversely

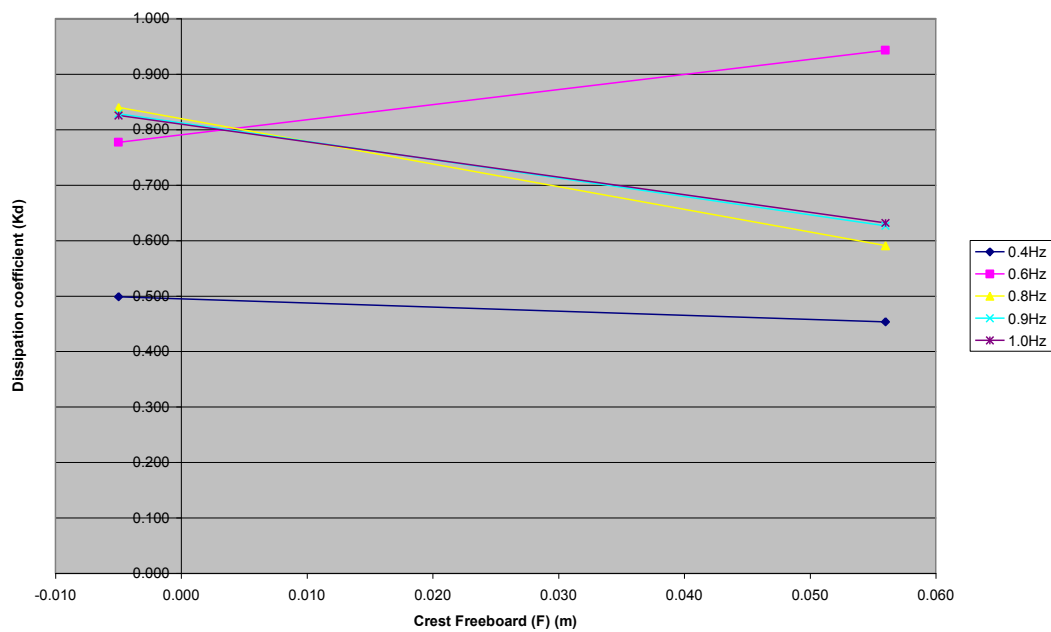


Figure 20: Dissipation coefficient (K_D) vs. Crest Freeboard (F) for different frequencies (gauge 5).

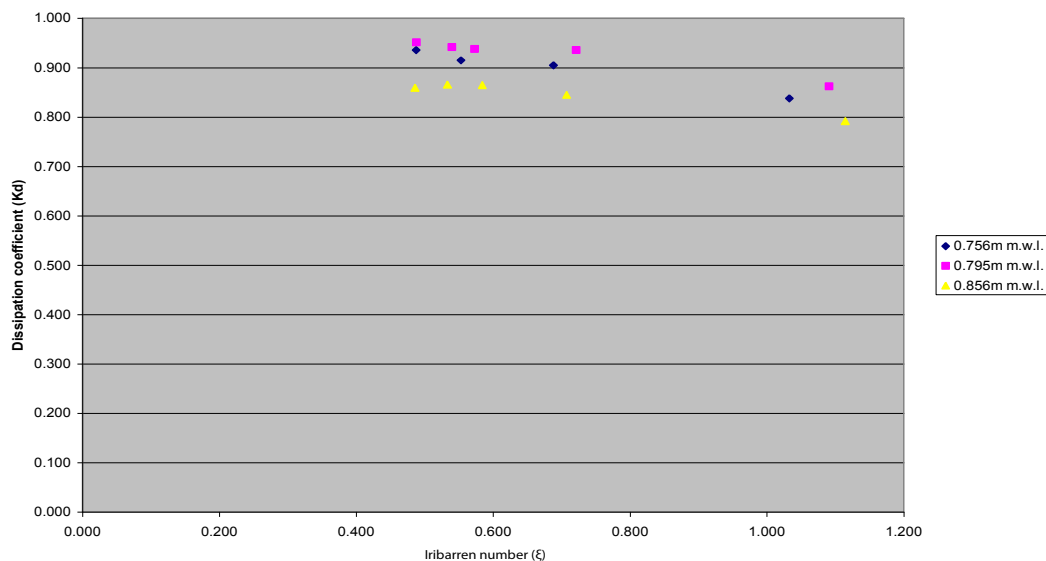
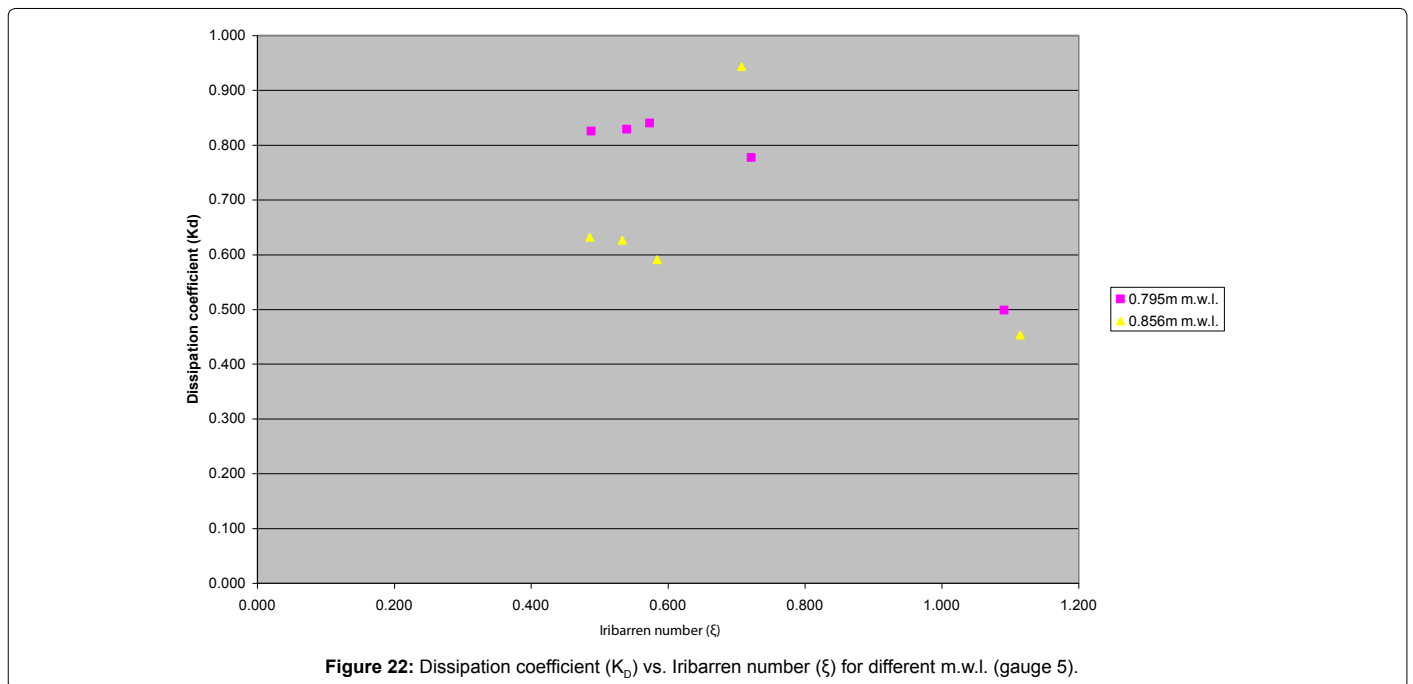


Figure 21: Dissipation coefficient (K_D) vs. Iribarren number (ξ) for different m.w.l. (gauge 4).



proportional to the increase of ξ . Furthermore, at gauge 5 there is again at $f=0.6$ Hz a changing point at the behavior of K_D .

Discussion

As the results were presented and were described in the previous section of this paper, their graphical presentation was not a helpful tool for analysis. The most accurate presentation, which can help to analyze and inform the discussion of the results, is the numerical presentation.

The low or high values of the reflection, transmission and dissipation coefficient was dependent on the fact that some waves (observed in the lab) were broken before reaching the model. The waves were broken at the two slopes before the model, and that was more noticeable at waves with high frequencies. As a result, they had hit the model with less energy than they had had in the beginning, due to the fact that it was already lost at the slopes. In summary, that energy was lost because of the bed friction and because of the production of turbulence. The bed friction was varied into the wave channel due to the fact that one part of the bed was made by wood (the sloping bed where the model was placed) and the rest by plastic.

In addition, the waves that broke in front and behind the model at its sloping bed created set-up and consequently produced an increase in the depth of the water above the still water level. This was marked more at the back side of the model when it was submerged. As well, the classic picture of a large wave curling over and breaking on the structure was rarely observed during this study. Possibly because of the sloping bed and the porous nature of the breakwater, waves appeared to be partly absorbed into the structure before they could break on it. This observation is in agreement with the Ahrens's (1984) observation at reef type breakwaters.

Furthermore, in the lab it was noticed that the waves which hit the slope behind the model were reflected back to the model causing some errors in the readings. The greatest errors were observed at waves with frequency equal to 0.4 Hz, which were the largest waves of the test that were generated, and these errors were shown also in the numerical

presentation of the results for both wave conditions. It was observed that an amount of volume of water flew out of the wave channel and this was not reflected at the slope at all.

From the investigation of the results taken from every gauge, it can be distinguished that the heights of waves at gauge 1 were slightly different from the gauges 2 and 3. This happened because of the fact that gauge 1 was placed at the flat bed of the wave channel instead of the gauges 2 and 3 which were placed at the sloping bed.

Additionally, the results from the general characteristics of waves at the gauges showed that celerity was inversely proportional with the increase of frequency and had greater values when the mean water level was raised. Also, when the waves reached the slope the celerity started to increase as they approached the model, in agreement with that reported by Yukiko T and Nobuhisa K [15].

Conclusion

Laboratory tests (experiment) were conducted to observe the performance of a reef breakwater model. The wave reflection, transmission and dissipation characteristics of the model were measured, with more interesting giving in the first two characteristics (K_r and K_t). The tests were carried out using constant crest width and height for a series of random wave conditions, with different mean water levels and different frequencies.

Furthermore, it can be seen from the results that the reflected and incident energy, as well as transmitted and incident energy, approximately cover the same frequency range. In general, the peak frequency of the reflected and transmitted waves appeared to be lower than the incident waves.

From the analysis, reflection coefficient has been shown to be a much more linear process than transmission. Reflection coefficient showed a systematic increase with the Iribarren number (ξ). However, the larger scatter in plots of K_r versus ξ (especially at regular waves) indicated that the Iribarren number does not represent the optimal mean for the description of the reflection process. In general, from the results of the

experiment, the reflection coefficient was also proportional to wave period (T), the deep-water wavelength (L_o), wavelength (L) and the significant incident wave height (H_{st}). Furthermore, K_r was inversely proportional to crest freeboard (F) and depth at the toe of the structure (d) as the model became submerged.

Transmission coefficient has shown that was not as much linear as reflection coefficient was, depending more on the crest freeboard (F). From the results, it can be observed that K_t was proportional with F , relative depth of crest freeboard (F/d), relative crest freeboard (F/H) and to F/L . However, in some cases the behavior of the transmission coefficient was changed as the model became submerged.

The K_t was proportional with the relative water depth (d/L) as the model became submerged. This is expected because larger values of d/L correspond to relatively deeper water waves, where in more energy is concentrated near the surface. When the relative depth of crest freeboard (F/d) is also large, this energy concentrated near the surface is easily transmitted across the structure.

The transmission coefficient was also proportional with frequency (f) and wave steepness (H/L) as the model became submerged. Nevertheless, the K_t became inversely proportional, as the model became submerged, with significant incident wave height (H_{st}), deep-water wavelength (L_o) and wavelength (L).

As far as dissipation is concerned, its value depends on the K_r and K_t since $K_D = 1 - K_r - K_t$. It was found that K_D was proportional to the frequency (f) and inversely proportional to the Iribarren number (ξ). However, the influence of the dissipation coefficient by the crest freeboard parameter was having exactly inverse results.

Acknowledgment

I would especially like to thank Professor G. N. Bullock for his encouragement and support.

References

1. Liu PLF (1994) *Advances in coastal and Ocean Engineering*. Singapore: World Scientific 1: 257-292.

2. Wamsley TV, Ahrens JP (2003) Computation of wave transmission coefficient at detached breakwaters for shoreline response modeling. *Proceedings of Coastal Structures*. 593-605.
3. Hornack M (2011) *Wave Reflection Characteristics of Permeable and Impermeable Submerged Trapezoidal Breakwaters*. All theses 1057.
4. Yulastuti DI, Hashim AM (2011) *Wave Transmission on Submerged Rubble Mound Breakwater Using L-Blocks*. 2nd International Conference on Environmental Science and Technology IPCBBE 6: 243- 248.
5. D'Angremond K, Van der Meer JW, De Jong RJ (1996) *Wave Transmission at Low-crested Structures*. *Proceedings of the 25th In. Conf. Coast. Engineering* 2418-2427.
6. Seabrook SR, Hall KR (1996) *Wave Transmission at Submerged Breakwaters*. *Proceedings of the 26th International Conference Coastal Engineering 2000-2013*. Denmark.
7. Friebel HC, Harris LE (2003) *Re-evaluation of Wave Transmission Coefficient Formulae from Submerged Breakwater Physical Model, Florida*.
8. Buccino M, Clabrese M (2007) *Conceptual Approach for Prediction of Wave Transmission at Low-crested Breakwater*. *Journal of Waterway, Port, Coastal and Ocean Engineering* 133: 213-224.
9. Buccino M, Del Vita I, Calabrese M (2013) *Predicting wave transmission past Reef Ball™ submerged breakwaters*. *Proceedings 12th International Coastal Symposium (Plymouth, England)*. *Journal of Coastal Research* 65: 171-176.
10. Ahrens JP (1984) *Reef Type Breakwaters*. *Proceedings of 19th International Conference on Coastal Engineering*. 3: 2648-2662.
11. Kobayashi N, Pietropaolo J, Melby J (2013) *Deformation of Reef Breakwaters and Wave Transmission*. *J Waterway Port Coastal Ocean Eng* 139: 336-340.
12. CIRIA/CUR (1991) *Manual on the use of rock in coastal and shoreline engineering*. London: CIRIA. 351-354.
13. Hughes SA (1993) *Physical Models and Laboratory Techniques in Coastal Engineering*. *Advanced Series on Ocean Engineering*. Singapore.
14. Sastry VSLNS, Holscher P, Barends FBJ (1991) *Numerical determination of wave transmission through a rubblemound breakwater at Visakhapatnam India*. *Journal of Coastal Engineering* 15: 41-57.
15. Yukiko T, Nobuhisa K (1999) *Stability of low rubble-mound under wave-current interaction*. *Coastal Structures-99*. 2: 713-720.